Clustering: a rational design principle for potentiated antibody therapeutics

Oostindie, S.C.

2

CD20 AND CD37 ANTIBODIES SYNERGIZE TO ACTIVATE COMPLEMENT BY FC-MEDIATED CLUSTERING

Simone C. Oostindie,[1,2,@] Hilma J. van der Horst,[3] Margaret A. Lindorfer,[4] Erika M. Cook,[4] Jillian C. Tupitza,[4] Clive S. Zent,[5] Richard Burack,[5] Karl R. VanDerMeid,[5] Kristin Strumane,[1] Martine E. D. Chamuleau,[3] Tuna Mutis,[3] Rob N. de Jong,[1] Janine Schuurman,[1] Esther C. W. Breij,[1] Frank J. Beurskens,[1] Paul W. H. I. Parren,[2,6] and Ronald P. Taylor[4,@]

Haematologica 2019 Sep;104(9):1841-1852.

1 Genmab, Utrecht, The Netherlands;
2 Department of Immunohematology and Blood Transfusion, Leiden University Medical Center, Leiden, The Netherlands;
3 Department of Hematology, Amsterdam University Medical Center, Amsterdam, The Netherlands;
4 Department of Biochemistry and Molecular Genetics, University of Virginia School of Medicine, Charlottesville, Virginia, USA;
5 Wilmot Cancer Institute, University of Rochester Medical Center, Rochester, New York, USA;
6 Lava Therapeutics, Utrecht, The Netherlands;
@ Corresponding author

Corresponding authors

Simone C. Oostindie, Genmab, Uppsalalaan 15, 3584CT, Utrecht, The Netherlands; e-mail: sio@genmab.com; and **Ronald P. Taylor**, Department of Biochemistry and Molecular Genetics, Box 800733, University of Virginia School of Medicine, Charlottesville, Virginia, 22908, USA; e-mail: rpt@virginia.edu

Acknowledgements

The authors would like to thank Joost Bakker (SCICOMVISUALS) for designing Figure 7.

ABSTRACT

CD20 monoclonal antibody therapies have significantly improved the outlook for patients with B-cell malignancies. However many patients acquire resistance, demonstrating the need for new and improved drugs. We previously demonstrated that the natural process of antibody hexamer formation on targeted cells allows for optimal induction of complement-dependent cytotoxicity. Complement-dependent cytotoxicity can be potentiated by introducing a single point mutation such as E430G in the IgG Fc domain that enhances intermolecular Fc-Fc interactions between cell-bound IgG molecules, thereby facilitating IgG hexamer formation. Antibodies specific for CD37, a target that is abundantly expressed on healthy and malignant B cells, are generally poor inducers of complement-dependent cytotoxicity. Here we demonstrate that introduction of the hexamerization-enhancing mutation E430G in CD37-specific antibodies facilitates highly potent complement-dependent cytotoxicity in chronic lymphocytic leukemia cells *ex vivo*. Strikingly, we observed that combinations of hexamerization-enhanced CD20 and CD37 antibodies cooperated in C1q binding and induced superior and synergistic complement-dependent cytotoxicity in patient-derived cancer cells compared to the single agents. Furthermore, CD20 and CD37 antibodies colocalized on the cell membrane, an effect that was potentiated by the hexamerization-enhancing mutation. Moreover, upon cell surface binding, CD20 and CD37 antibodies were shown to form mixed hexameric antibody complexes consisting of both antibodies each bound to their own cognate target, so-called hetero-hexamers. These findings give novel insights into the mechanisms of synergy in antibody-mediated complement-dependent cytotoxicity and provide a rationale to explore Fc-engineering and antibody hetero-hexamerization as a tool to enhance the cooperativity and therapeutic efficacy of antibody combinations.

INTRODUCTION

Monoclonal antibodies (mAbs) have become the backbone of treatment regimens for several cancer indications. The chimeric immunoglobulin (Ig) G1 CD20 mAb rituximab was the first mAb approved for clinical use in cancer therapy. CD20 is expressed on more than 90% of mature B cells and rituximab is widely used to treat B-cell malignancies.[1-3] However, many patients do not experience complete remission or acquire resistance to rituximab treatment, thereby demonstrating the need for improved mAb therapeutics or alternative tumor-targeting strategies.[4-6]

mAbs employ various mechanisms to eliminate cancer cells, such as induction of programmed cell death or Fc-mediated effector functions, including antibody-dependent cell-mediated cytotoxicity (ADCC), antibody-dependent cellular phagocytosis (ADCP) and complement-dependent cytotoxicity (CDC), which can be increased by Fc engineering.[7] ADCC and ADCP, for example, can be enhanced by improving FcγR binding through Fc glyco-engineering or amino acid modifications.[8-11] Likewise, C1q binding and CDC can be increased by amino acid substitutions in Fc domains.[12,13] CDC is initiated when membrane-bound antibodies bind the hexavalent C1q molecule, which together with C1r and C1s forms the C1 complex, the first component of the classical complement pathway. C1 activation triggers an enzymatic cascade that leads to covalent attachment of opsonins to target cells, and the generation of potent chemo attractants, anaphylatoxins and membrane attack complexes (MACs).[14] IgG antibodies bound to cell surface antigens assemble into ordered hexamers, providing high avidity docking sites to which C1 binds and is activated.[15] IgG hexamer formation and complement activation can be enhanced by single point mutations in IgG Fc domains, such as E430G, which increase interactions between Fc domains of cell-bound IgG.[16] The hexamerization-enhanced (Hx) CD20-targeting mAb 7D8 displayed strongly enhanced CDC of B cells from patients with chronic lymphocytic leukemia (CLL), which often demonstrate complement resistance due to low CD20 and high membrane complement regulatory protein (mCRP) expression.[16-18]

In polyclonal antibody responses, antibodies against distinct epitopes or antigens are thought to cooperate resulting in increased effector functions against target cells. This increase can be mimicked in mAb combinations or cocktails. For example, monoclonal EGFR antibodies do not induce CDC *in vitro*, but combinations of mAbs against multiple EGFR epitopes induced potent CDC.[19,20]

CD37, which is abundantly expressed on B cells, represents a promising therapeutic target for the treatment of B-cell malignancies.[21,22] Currently known CD37 mAbs in clinical development however, are generally poor inducers of CDC.[23-27] Here we show that introducing Hx mutations into CD37 mAbs strongly potentiated CDC of CLL cells, and that combinations of CD20 and CD37 targeting mAbs could further enhance CDC of tumor cell lines and primary patient cells. We investigated the mechanism behind the synergistic CDC activity of CD20 and CD37 mAbs, and found that the mAb combinations activate complement cooperatively. The two mAbs formed mixed hexameric antibody complexes consisting of both antibodies each bound to their cognate targets, which we termed hetero-hexamers. The concept of hetero-hexamer formation and the use of Fc-Fc interaction enhancing mutations could serve as a tool to enhance cooperativity, and thereby the tumor killing capacity, of mAb combinations.

METHODS

Cells

Daudi, Raji and WIL2-S B-lymphoma cell lines were obtained from the American Type Culture Collection (ATCC no. CCL-213, CCL-86 and CRL-8885 respectively). All primary patient cells used in this study were obtained after written and informed consent and stored using protocols approved by the institutional review boards in accordance with the declaration of Helsinki (see Online Supplementary Methods).

Antibodies and reagents

mAbs IgG1-CD20-7D8, IgG1-CD20-11B8, IgG1-CD37 clone 37.3 and IgG1-gp120 were recombinantly produced at Genmab.[18,28-30] The HIV-1 gp120 mAb b12 was used to determine assay background signal. Mutations to enhance or inhibit Fc-Fc interactions were introduced in expression vectors encoding the antibody heavy chain by gene synthesis (GeneArt). Rituximab (MabThera®), ofatumumab (Arzerra®) and obinutuzumab (Gazyvaro®) were obtained from the pharmacy (UMC Utrecht). See Online Supplementary Methods for details on reagents used.

CDC assays

CDC assays with CLL patient cells were performed with human complement as described.[31] CDC assays with B-lymphoma cell lines and patient-derived B-lymphoma cells were performed using 100,000 target cells incubated (45 minutes at 37˚C) with a mAb concentration series and pooled normal human serum (NHS, 20% final concentration) as a complement source. Killing was calculated as the percentage of propidium idodide (PI) or 7-AAD positive cells determined by flow cytometry. See Online Supplementary Methods for details on cell markers used to define cell populations.

Expression analysis

Expression levels of cellular markers were determined using an indirect immunofluorescence assay (QIFIKIT®, Agilent Technologies) according to the manufacturer's instructions (see online Supplementary Methods).

C1q binding and CDC efficacy

Daudi cells (3 x 10^6 cells/mL) were incubated with 10 µg/mL mAb and a concentration series of purified human C1q for 45 minutes at 37˚C. After washing, cells were incubated with FITC-labeled rabbit anti-human C1q antibody for 30 minutes at 4˚C and analyzed on a FACS Canto II flow cytometer (BD Biosciences, CA, USA). The efficiency of C1q binding and subsequent CDC was

assessed as described above using fixed mAb concentrations, a concentration series of purified C1q and 20% C1q depleted serum.

Confocal microscopy

Raji cells were opsonized with A488 labeled Hx-CD20-7D8 and A594 labeled Hx-CD37 mAbs (2.5 µg/mL final concentrations), and incubated for 15 minutes at room temperature. After washing, cells were placed on a poly-D lysine-coated slide and images were captured with a Zeiss AxioObserver LSM 700 microscope using plan-Apochromat 63X/1.40 Oil DIC M27 objective lenses and acquired/processed using Zen software.

Förster Resonance Energy Transfer (FRET) analysis

Proximity-induced FRET was determined by measuring energy transfer between cells incubated with A555-conjugated donor and A647-conjugated acceptor mAbs using flow cytometry (see Online Supplementary Methods). The dynamic range of FRET analysis by flow cytometry was determined using control mAbs, as specified in Supplementary Figure 1.

Data processing and statistical analyses

All values are expressed as the mean ± standard deviation of at least two independent experiments. Graphs were generated and analyzed using GraphPad Prism 7.0 (CA, USA). Differences between two groups were analyzed using paired Student's t-test with two-tailed 95% confidence intervals and between more groups by paired or unpaired one-way ANOVA followed by a Tukey post-hoc multiple comparisons test. Significant differences are indicated as: *$p < 0.05$, **$p < 0.01$, ***$p < 0.001$ and ****$p < 0.0001$. See Online Supplementary Methods for details on synergy and colocalization analysis.

RESULTS

Hexamerization-enhancing mutations in CD20 and CD37 mAbs substantially enhance CDC of CLL B cells

We previously reported increased CDC with engineered mAbs containing Hx mutations in the Fc domain.[15,16] We therefore investigated whether introducing the Hx mutation E430G into the CD37 chimeric IgG1 mAb 37.3 could potentiate CDC in B cells isolated from CLL patients and compared this to the CD20 mAb IgG1-CD20-7D8 with and without a Hx mutation. Wild-type (WT) IgG1-CD20-7D8 promoted considerable CDC of CLL B cells and CDC was increased by the E430G mutation (Figure 1A). While WT IgG1-CD37 efficiently binds to CLL B cells, it was ineffective at inducing CDC (Figure 1B; Supplementary Figure 2), in contrast to Hx-CD37 (Figure 1B). For both Hx-CD20-7D8 and Hx-CD37, high levels of cell killing largely required active complement, since CDC was almost absent in heat-inactivated NHS, NHS supplemented with EDTA or medium alone (Figure 1 A-B). Background killing of cells from patient A mediated by Hx-CD37 in the absence of complement was slightly higher than expected. However, in C1q-depleted serum, background killing was 16%, compared to 6% for cells reacted with Hx-CD20-7D8. Background killing in C1q-depleted serum for 6 other CLL patient samples averaged 13% and 14% for cells reacted with Hx-CD20-7D8 and Hx-CD37, respectively. Reaction in NHS increased CDC to averages of 91% and 95%, respectively. Introduction of the Hx mutation E430G into CD20 and CD37 mAbs did not affect pharmacokinetic profiles and binding to FcRn (data not shown).[16] At the highest concentration (16 µg/mL) Hx-CD37 induced ≥ 95% CDC of tumor B cells for 9 out of 12 patients (Figure 1C). At concentrations of 0.25 and 2 µg/mL, Hx-CD37 generally demonstrated higher potency than Hx-CD20-7D8 (Figure 1D-E), which may be explained by higher expression levels of CD37 (approximately 2-fold) in the majority of CLL samples (Supplementary Figure 3A-B).

CD20 and CD37 mAbs synergistically induce CDC of malignant B cells

We investigated the CDC activity of combinations of WT CD20 and WT CD37 mAbs, using two different CD20 mAbs. The ability to activate complement represents a key distinction between type I CD20 mAbs which mediate strong CDC and type II CD20 mAbs, which only mediate weak CDC.[32] The effect of combining WT type I CD20 mAb 7D8 or WT type II CD20 mAb 11B8 with WT CD37 mAb on CDC was assessed using Daudi cells. As expected, WT IgG1-CD20-7D8 showed potent CDC activity (96.6% cell lysis), whereas WT IgG1-CD37 did not induce CDC (Figure 2A). The combination of WT IgG1-CD20-7D8 and WT IgG1-CD37 did not demonstrate enhanced CDC. However, while neither WT IgG1-CD20-11B8 nor WT IgG1-CD37 induced CDC as single agents, the combination

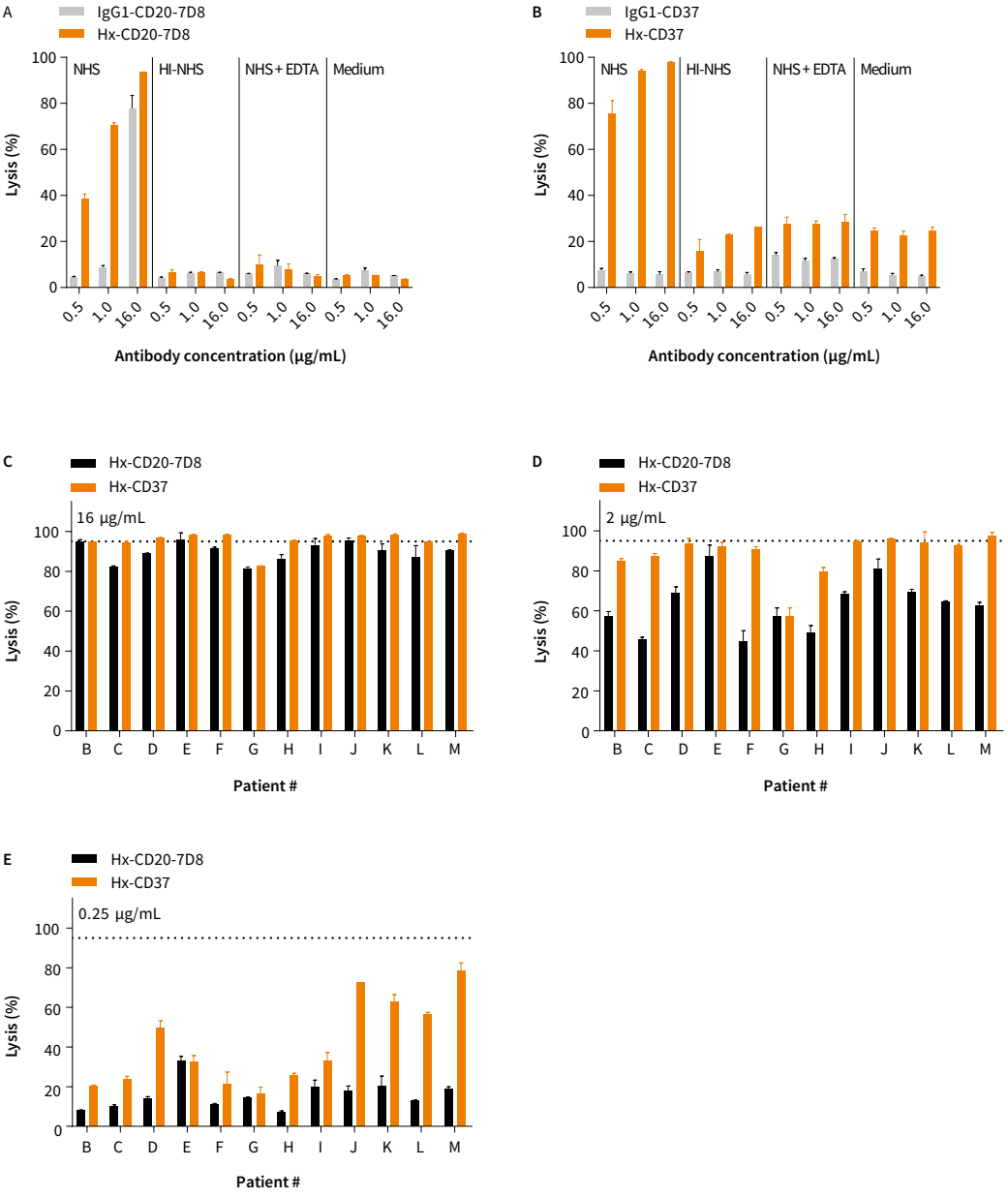

▲ **Figure 1**

Hexamerization-enhancing mutations in CD20 and CD37 mAbs substantially enhance CDC of CLL B cells.
(**A**-**B**) CDC of B cells obtained from patient A with CLL. Cells were opsonized with different concentrations of CD20 mAb 7D8 as wild type (IgG1-CD20-7D8) or with a hexamerization-enhancing mutation (Hx-CD20-7D8) (**A**); or CD37 mAb 37.3 as wild type (IgG1-CD37) or with a hexamerization-enhancing mutation (Hx-CD37) (**B**) in the presence of 50% pooled normal human serum (NHS), heat-inactivated (HI) NHS, NHS + EDTA or medium. Representative examples of three replicate experiments are shown. (**C**-**E**) CDC of B cells obtained from 12 different CLL patients (patient B-M). CLL B cells were opsonized with 16 µg/mL (**C**), 2 µg/mL (**D**) or 0.25 µg/mL (**E**) Hx-CD20-7D8 or Hx-CD37. The dashed line represents 95% cell lysis. CDC induction is expressed as the percentage lysis determined by the fraction of TO-PRO-3 positive cells and data shown are mean and standard deviation (SD) of duplicate measurements.

promoted strong lysis of approximately 60% (Figure 2B). Minimal cell lysis was observed in experiments with heat-inactivated serum, indicating that that cell killing was largely dependent on complement (Supplementary Figure 4).

We additionally examined whether combinations of CD20 and CD37 mAbs with Hx mutations also showed cooperativity in CDC by testing mAb combinations using a full dose-response matrix (8x8 serial dilution grid) based on the EC50 values of the single mAbs. Surprisingly, both Hx-CD20-7D8 and Hx-CD20-11B8 in combination with Hx-CD37 showed enhanced CDC of Daudi cells compared to the single agents (Figure 2C, Supplementary Figure 5A). We next assessed whether the observed combination effect was synergistic using the Loewe additivity-based combination index (CI) score calculated by CompuSyn, whereby effects were categorized as synergistic (CI < 1), additive (CI = 1) or antagonistic (CI > 1).[33] The Loewe additivity-based model assumes synergy when the effect of a drug combination is higher than the effect of a drug combined with itself, and takes into account both the potency and the shape of the dose-effect curve of each drug in the dose-response matrix. Synergy was observed for both Hx-CD20-7D8 and Hx-CD20-11B8 when combined with Hx-CD37, with average CI values of 0.37 and 0.31 (effective dose - ED95), respectively (Figure 2D, Supplementary Figure 5B, Supplementary Table 1). At the lower tested mAb concentrations, synergy was more profound (lower CI values) for combinations of Hx-CD37 with type II CD20 mAb-derived Hx-CD20-11B8 than with type I CD20 mAb-derived Hx-CD20-7D8.

In addition to Daudi cells, we used two other B-cell lines expressing various levels of CD20 and CD37 to further examine the cooperativity in CDC between combinations of Hx-CD37 with Hx-CD20 mAbs or with clinically validated CD20 mAbs. Across all B-cell lines tested, enhanced CDC activity was observed for

Figure 2 ►

CD20 and CD37 mAbs synergistically induce CDC of malignant B cells.
(**A-B**) CDC on Daudi cells opsonized with 30 µg/mL WT type I CD20 mAb 7D8 (IgG1-CD20-7D8) (**A**) or type II CD20 mAb 11B8 (IgG1-CD20-11B8) (**B**), CD37 mAb 37.3 (IgG1-CD37), or a combination thereof (15 + 15 µg/mL) in the presence of 20% NHS. CDC induction is expressed as the percentage lysis determined by the fraction of propidium iodide (PI)-positive cells. Data shown are mean and SD of triplicate measurements. (**C**) 8 x 8 CDC dose response matrix plot for the combination of hexamerization-enhanced CD37 mAb Hx-CD37 (0-0.8 µg/mL) with hexamerization-enhanced CD20 mAb Hx-CD20-11B8 (0-8 µg/mL), tested on Daudi cells and categorized as a color gradient from green (0% lysis) to yellow (50% lysis) to red (100% lysis). HIV gp120-specific mAb b12 (IgG1-gp120) was used as a negative control human mAb. (**D**) Loewe additivity-based Combination index (CI) values calculated by CompuSyn for the CDC dose response matrix as described in (**C**) and categorized as synergistic (<1, red), additive (1, white) and antagonistic (>1, blue). Representative examples of two replicate experiments are shown. (**E**) CDC and CD37 expression analysis on Daudi, Raji and WIL2-S cells. For the CDC assay, cells were opsonized with Hx-CD37 (10 µg/mL), different CD20 mAb variants (10 µg/mL) or combinations thereof (10 + 10 µg/mL). Data show the mean of nine replicates collected from three independent experiments. Expression levels were determined using QIFIKIT analysis. The number of antibody molecules per cell was calculated from the antibody-binding capacity (mean fluorescence intensity - MFI) normalized to a calibration curve, according to the manufacturer's guidelines. Expression data show the mean of four replicates collected from two independent experiments.

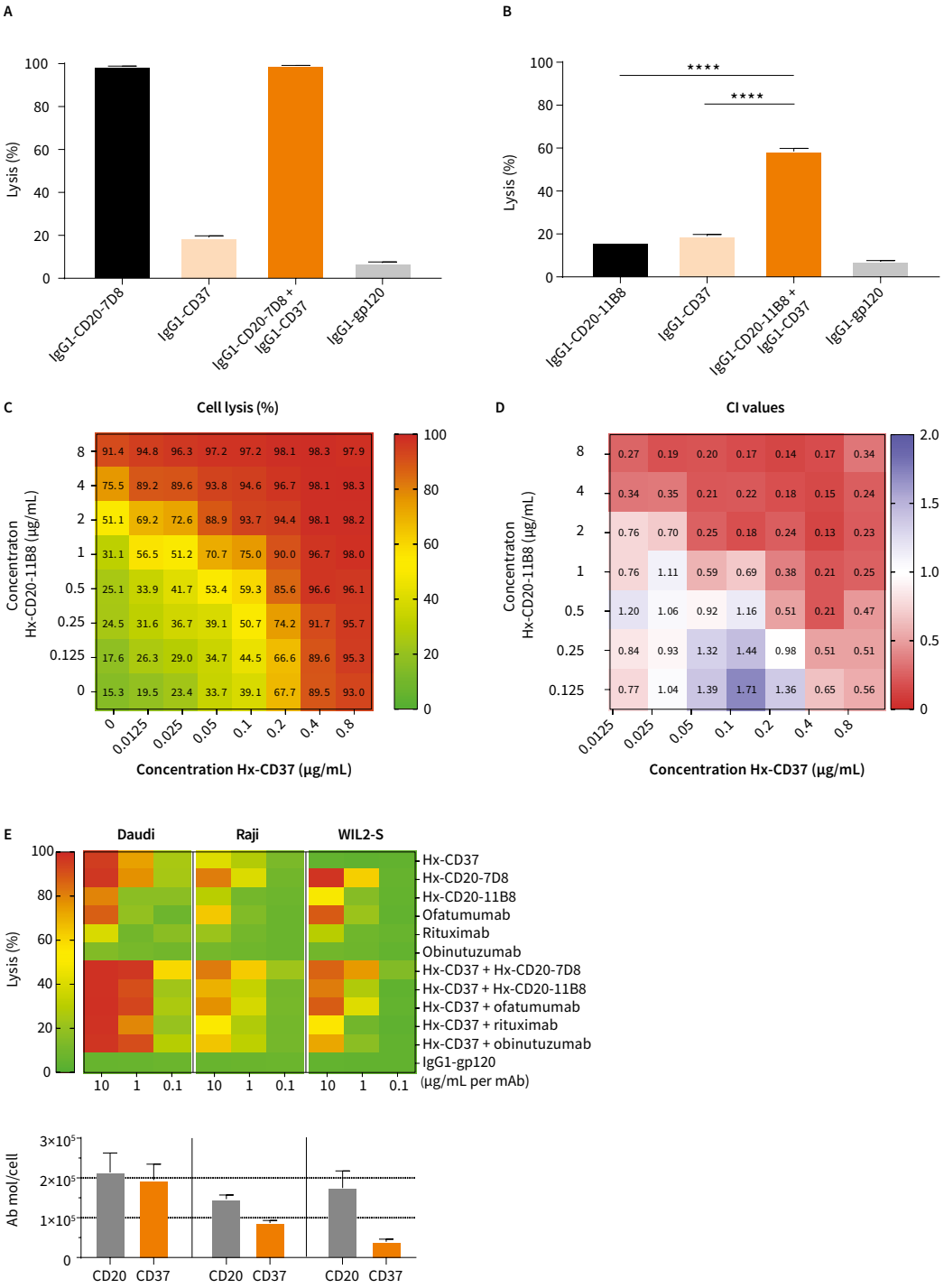
A
Lysis (%)
IgG1-CD20-7D8
IgG1-CD37
IgG1-CD20-7D8 + IgG1-CD37
IgG1-gp120
B
****
****
Lysis (%)
IgG1-CD20-11B8
IgG1-CD37
IgG1-CD20-11B8 + IgG1-CD37
IgG1-gp120
C
Cell lysis (%)
Concentraton Hx-CD20-11B8 (µg/mL)
Concentration Hx-CD37 (µg/mL)
D
CI values
Concentraton Hx-CD20-11B8 (µg/mL)
Concentration Hx-CD37 (µg/mL)
E
Daudi
Raji
WIL2-S
Lysis (%)
Hx-CD37
Hx-CD20-7D8
Hx-CD20-11B8
Ofatumumab
Rituximab
Obinutuzumab
Hx-CD37 + Hx-CD20-7D8
Hx-CD37 + Hx-CD20-11B8
Hx-CD37 + ofatumumab
Hx-CD37 + rituximab
Hx-CD37 + obinutuzumab
IgG1-gp120
(µg/mL per mAb)
Ab mol/cell
CD20 CD37 CD20 CD37 CD20 CD37

combinations of Hx-CD37 with Hx-CD20 mAbs, as well as for combinations of Hx-CD37 with ofatumumab, rituximab and obinutuzumab (Figure 2E). Even in WIL2-S cells expressing low levels of CD37, a combination of Hx-CD37 with obinutuzumab induced 72% lysis, whereas the single agents induced only 5% and 10% lysis respectively. Despite high single agent activity of Hx-CD37 and Hx-CD20 mAbs at 10 µg/mL (per mAb) in Daudi cells, the cooperativity between Hx-CD37 and Hx-CD20 mAbs became apparent at the lower mAb concentrations.

Enhanced binding and use of C1q by combinations of hexamerization-enhanced CD20 and CD37 mAbs

We hypothesized that the observed synergy in CDC between Hx-CD20 and Hx-CD37 mAbs resulted from more efficient use of complement proteins, starting with binding of C1q. Therefore, we determined whether combinations of Hx-CD20 and Hx-CD37 differed in their C1q binding capacity. We incubated Daudi cells with fixed mAb concentrations and titrated C1q, and measured C1q binding and the concentration of C1q required to induce CDC, referred to here as CDC efficacy. Hx-CD20-7D8 already induced efficient C1q binding as a single agent, while Hx-CD37 showed limited C1q binding (Figure 3A). Combinations of Hx-CD20-7D8 and Hx-CD37 did not significantly increase C1q binding. However, the combination showed higher CDC efficacy as demonstrated by the lower EC50 value in the C1q dose-response curves compared to the single mAbs (0.03 µg/mL for the combination versus 0.12 µg/mL for Hx-CD20-7D8 and 0.34 µg/mL for Hx-CD20-11B8) (Figure 3B). In contrast to the results with the type I CD20 mAb-derived variant, combining type II CD20 mAb-derived Hx-CD20-11B8 with Hx-CD37 resulted in increased C1q binding compared to the single mAbs, as well as increased CDC efficacy (Figure 3C-D). Collectively, these data suggest that combinations of both type I and type II CD20 mAb-derived Hx-CD20 mAbs with Hx-CD37 mAbs activate complement more effectively.

CD20 and CD37 mAbs colocalize on B cells

Confocal microscopy was used to determine whether the CD20- and CD37-specific antibodies associate on the cell surface upon target binding. Cell-bound Hx variants of CD20 mAb 7D8 and CD37 mAb 37.3 were detected using A488 and A594 fluorescent labeling, respectively, and antibody colocalization was quantified by calculating spatial overlap (Manders' coefficients) between the two fluorescent labels. The merged A488/A594 image showed that membrane-bound Hx-CD20 and Hx-CD37 mAbs indeed colocalized on the surface of Raji cells (Figure 4A), which was confirmed by quantitative analysis, giving Manders' Coefficients of M1=0.805 (fraction of image 1 overlapping image 2) and M2=0.751 (fraction of image 2 overlapping image 1).

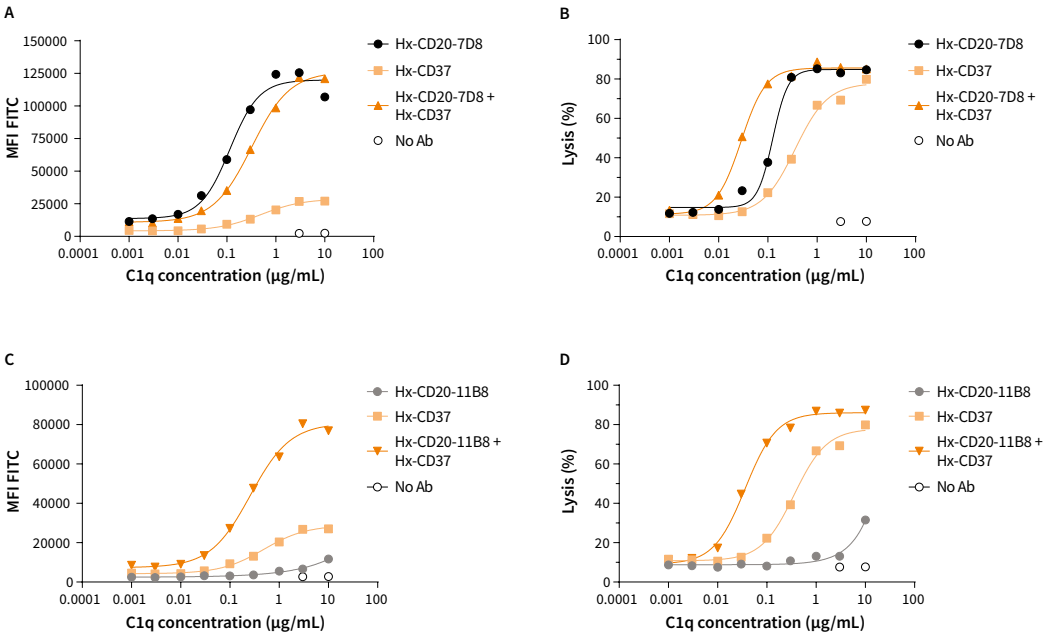

▲ **Figure 3**

Enhanced binding and use of C1q by combinations of hexamerization-enhanced CD20 and CD37 mAbs.
The capacity to bind C1q (**A, C**) and the efficiency to bind C1q and promote CDC (**B, D**) was assessed using Daudi cells opsonized with 10 µg/mL of hexamerization-enhanced variants of type I CD20 mAb-derived Hx-CD20-7D8 (**A-B**) or type II CD20 mAb-derived Hx-CD20-11B8 (**C-D**), CD37 mAb 37.3-derived Hx-CD37, or a combination thereof (5 + 5 µg/mL). Binding was detected using a FITC-labeled rabbit anti-human C1q secondary antibody and is expressed as MFI. CDC induction was assessed in C1q-depleted serum by calculating the percentage of PI-positive cells as determined by flow cytometry. Representative examples of three replicate experiments are shown.

Colocalization of cell-bound CD20 and CD37 mAbs was further examined by directly assessing molecular proximity using fluorescence resonance energy transfer (FRET) analysis. We examined FRET on Daudi cells between WT and Hx variants of CD20 and CD37 mAbs alone and in combination. Consistent with its CDC activity (Figure 2A), WT IgG1-CD20-7D8 induced high FRET, which suggests antibody hexamer formation (Figure 4B). WT IgG1-CD20-11B8 did not demonstrate proximity-induced FRET (Figure 4C), and WT IgG1-CD37 induced approximately 15% FRET (Figure 4B-C). Introducing a Hx mutation resulted in increased FRET levels for each of the single agents, indicating that enhancing Fc-Fc interactions increases mAb colocalization at the cell surface ($P<0.0001$, Figure 4D-E). Introduction of the Hx mutation did not affect target binding (data not shown), thereby excluding the possibility that increased FRET would be due to more mAbs being available on the cell surface. Combinations of WT IgG1-CD20-7D8 and WT IgG1-CD37 induced approximately 30% FRET, which was increased compared to the WT IgG1-CD37 single mAb ($P<0.0001$, Figure 4B). Combinations of WT IgG1-CD20-11B8 and WT IgG1-

A

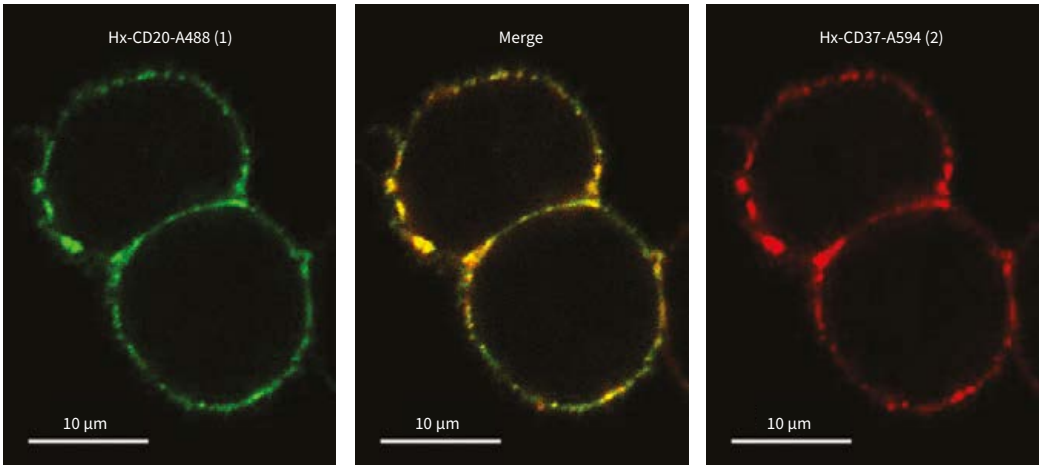

B

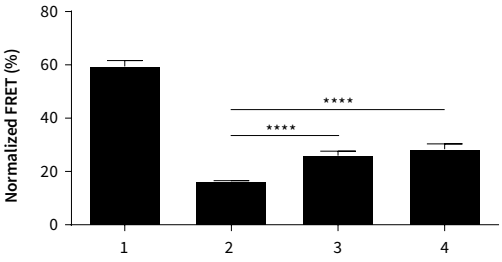

1. IgG1-CD20-7D8-A555 + IgG1-CD20-7D8-A647
2. IgG1-CD37-A555 + IgG1-CD37-A647
3. IgG1-CD20-7D8-A555 + IgG1-CD37-A647
4. IgG1-CD37-A555 + IgG1-CD20-7D8-A647

C

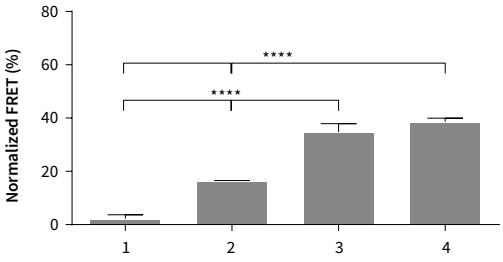

1. IgG1-CD20-11B8-A555 + IgG1-CD20-11B8-A647
2. IgG1-CD37-A555 + IgG1-CD37-A647
3. IgG1-CD20-11B8-A555 + IgG1-CD37-A647
4. IgG1-CD37-A555 + IgG1-CD20-11B8-A647

D

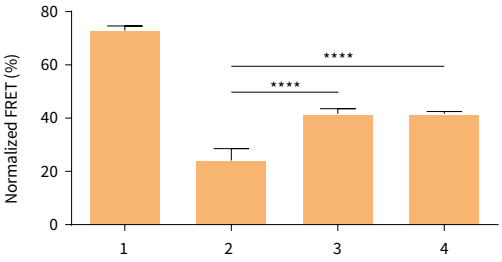

1. Hx-CD20-7D8-A555 + Hx-CD20-7D8-A647
2. Hx-CD37-A555 + Hx-CD37-A647
3. Hx-CD20-7D8-A555 + Hx-CD37-A647
4. Hx-CD37-A555 + Hx-CD20-7D8-A647

E

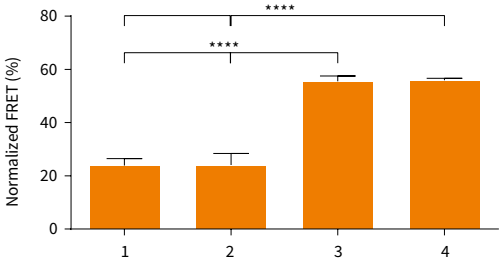

1. Hx-CD20-11B8-A555 + Hx-CD20-11B8-A647
2. Hx-CD37-A555 + Hx-CD37-A647
3. Hx-CD20-11B8-A555 + Hx-CD37-A647
4. Hx-CD37-A555 + Hx-CD20-11B8-A647

◀ **Figure 4**

CD20 and CD37 mAbs colocalize on B cells.

(**A**) Confocal fluorescence microscopy analysis to detect colocalization of cell-bound CD20 and CD37 mAbs. Raji cells were opsonized with hexamerization-enhanced A488-conjugated CD20 mAb 7D8-derived Hx-CD20-7D8 (image 1, green) and hexamerization-enhanced A594-conjugated CD37 mAb 37.3-derived Hx-CD37 (image 2, red), and incubated for 15 minutes at room temperature. Images were captured in PBS imaging medium at ambient temperature using a Zeiss AxioObserver LSM 700 microscope with Plan-Apochromat 63X/1.40 Oil DIC M27 objective lenses and acquired/processed using Zen software. Two excitation lasers were used at 488 and 555 nm. In the merged image, overlap of red and green produces orange or yellow. A representative example of two replicate experiments is shown. (**B-C**) FRET analysis to detect the molecular proximity of (**B**) WT type I CD20 mAb 7D8 (IgG1-CD20-7D8) or (**C**) WT type II CD20 mAb 11B8 (IgG1-CD20-11B8), WT CD37 mAb 37.3 (IgG1-CD37) or a combination thereof on the cell membrane of Daudi cells. (**D-E**) FRET analysis to detect the molecular proximity of hexamerization enhanced variants of (**D**) type I CD20 mAb 7D8-derived Hx-CD20-7D8 or (**E**) type II CD20 mAb 11B8-derived Hx-CD20-11B8, CD37 mAb 37.3-derived Hx-CD37 or a combination thereof on the cell membrane of Daudi cells. Daudi cells were opsonized with 10 µg/mL A555-conjugated- and 10 µg/mL A647-conjugated antibody variants for 15 minutes at 37˚C. FRET was calculated from MFI values as determined by flow cytometry. Data shown are mean and SD of six replicates collected from three independent experiments.

CD37 substantially increased FRET compared to each single mAb ($P < 0.0001$, Figure 4C), consistent with the enhanced CDC induction (Figure 2B). Combinations of Hx-CD20-7D8 or Hx-CD20-11B8 with Hx-CD37 further enhanced FRET compared to the FRET levels induced by the WT mAb combinations ($P<0.0001$, Figure 4D-E). These results confirm that CD20 and CD37 IgG1 mAbs bind in close proximity on the cell membrane, which can be enhanced by introducing the E430G mutation.

Hexamerization-enhanced CD20 and CD37 mAbs cooperate in CDC through Fc-mediated clustering in hetero-hexamers

Both enhancing Fc-Fc interactions in the CD20 or CD37 mAbs and combining the two B-cell target mAbs resulted in enhanced mAb colocalization. Together with the dependency of CDC on the formation of hexameric IgG complexes on the cell surface[15], this suggests that the CD20 and CD37 mAbs might not only form hexamers composed of mAbs bound to identical surface targets, but may cooperate by also forming mixed hexameric complexes of mAbs bound to either target, referred to here as hetero-hexamers. The contribution of Fc-Fc interactions between Hx-CD20-11B8 and Hx-CD37 to the CDC activity of the mAb combination was examined by the introduction of the complementary Fc-Fc interface mutations K439E and S440K. K439E and S440K suppress Fc-Fc interactions between antibody molecules containing the same mutation, whereas Fc-Fc interactions are restored in K439K and S440K antibody mixtures.[15] The capacity of Hx-CD20-11B8 and Hx-CD37 variants with K439E and S440K mutations to induce CDC was tested using Daudi and WIL2-S cells.

The CDC activity of Hx-CD20-11B8 was completely inhibited by introducing either the K439E or S440K Fc-Fc inhibiting mutation using Daudi and WIL2-S cells (Figure 5A-B). CDC activity was restored when Fc-Fc inhibition was

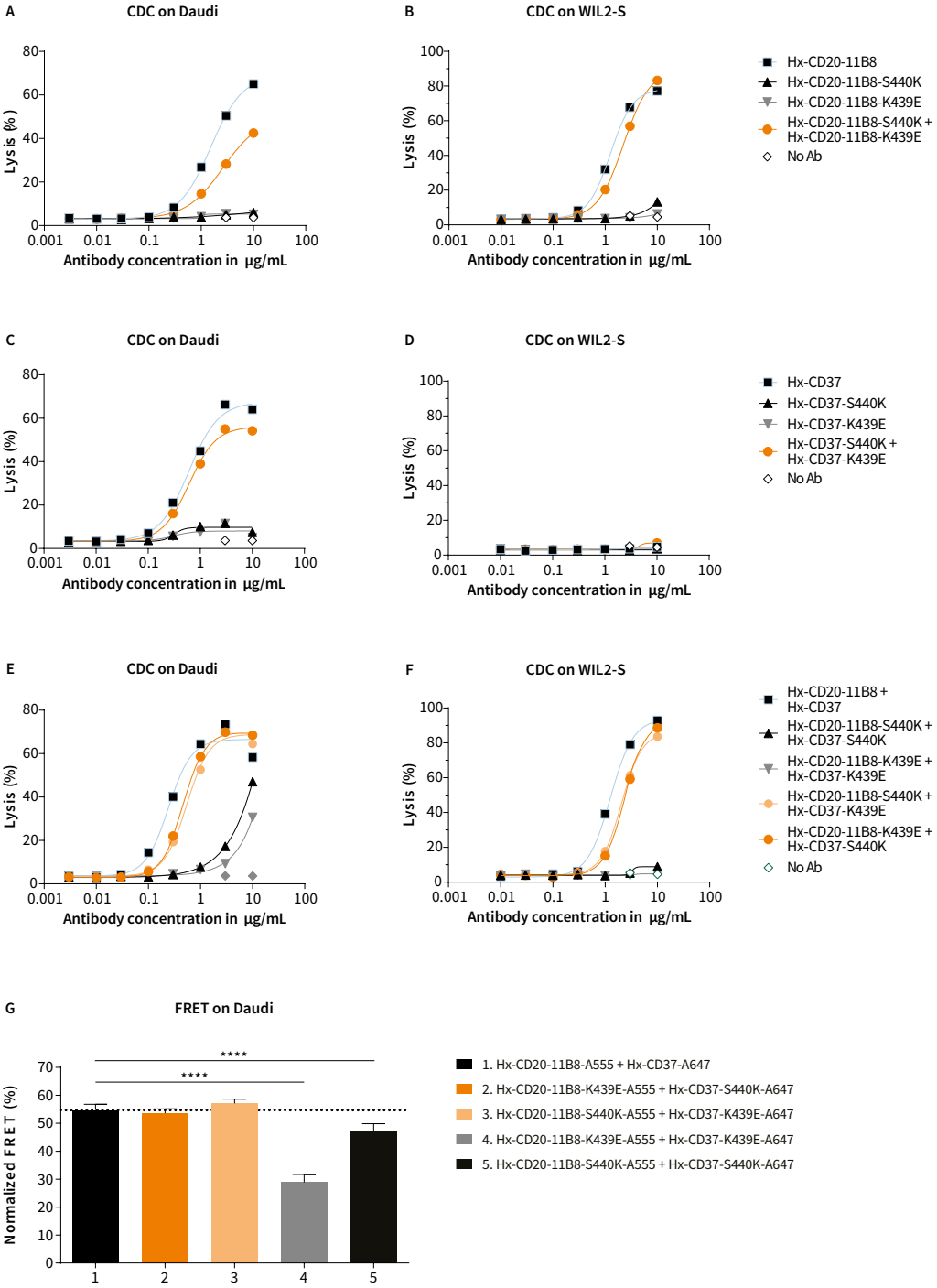
A
CDC on Daudi
Lysis (%)
Antibody concentration in µg/mL
B
CDC on WIL2-S
Lysis (%)
Antibody concentration in µg/mL
Hx-CD20-11B8
Hx-CD20-11B8-S440K
Hx-CD20-11B8-K439E
Hx-CD20-11B8-S440K + Hx-CD20-11B8-K439E
No Ab
C
CDC on Daudi
Lysis (%)
Antibody concentration in µg/mL
D
CDC on WIL2-S
Lysis (%)
Antibody concentration in µg/mL
Hx-CD37
Hx-CD37-S440K
Hx-CD37-K439E
Hx-CD37-S440K + Hx-CD37-K439E
No Ab
E
CDC on Daudi
Lysis (%)
Antibody concentration in µg/mL
F
CDC on WIL2-S
Lysis (%)
Antibody concentration in µg/mL
Hx-CD20-11B8 + Hx-CD37
Hx-CD20-11B8-S440K + Hx-CD37-S440K
Hx-CD20-11B8-K439E + Hx-CD37-K439E
Hx-CD20-11B8-S440K + Hx-CD37-K439E
Hx-CD20-11B8-K439E + Hx-CD37-S440K
No Ab
G
FRET on Daudi
Normalized FRET (%)
****
****
1. Hx-CD20-11B8-A555 + Hx-CD37-A647
2. Hx-CD20-11B8-K439E-A555 + Hx-CD37-S440K-A647
3. Hx-CD20-11B8-S440K-A555 + Hx-CD37-K439E-A647
4. Hx-CD20-11B8-K439E-A555 + Hx-CD37-K439E-A647
5. Hx-CD20-11B8-S440K-A555 + Hx-CD37-S440K-A647

neutralized by mixing the two CD20 mAbs. Similar results were observed for Hx-CD37 on Daudi cells, while on WIL2-S cells, Hx-CD37 did not induce CDC, most likely due to low CD37 expression (Figure 5C-D). Combining Hx-CD20-11B8 and Hx-CD37 mAbs harboring the same Fc-Fc inhibiting mutation (K439E or S440K) strongly reduced CDC activity on Daudi and WIL2-S cells (Figure 5E-F). However, CDC of both cell lines was restored by mixing Hx-CD20-11B8 and Hx-CD37, each carrying one of the complementary mutations K439E or S440K. These data suggest that Hx-CD20-11B8 and Hx-CD37 can indeed form hetero-hexameric complexes, thereby cooperating to activate complement.

Next, the effect of the Fc-Fc interaction-inhibiting mutations on colocalization of Hx-CD20-11B8 and Hx-CD37 mAbs on the cell membrane of Daudi cells was evaluated using FRET analysis. mAb combinations with Hx-CD20-11B8 and Hx-CD37 variants, both harboring the same Fc-Fc inhibiting mutation (K439E or S440K) showed reduced FRET on Daudi cells (Figure 5G; Supplementary Figure 6). FRET levels were restored when Fc-Fc inhibition was neutralized by combining Hx-CD20-11B8 and Hx-CD37 mAbs, each having one of the complementary mutations K439E or S440K. Thus, donor- and acceptor-labeled Hx-CD20-11B8 and Hx-CD37 mAb variants come together in close proximity on the cell membrane of Daudi cells, which appears to be, at least in part, mediated by the Fc domain.

Combinations of hexamerization-enhanced CD20 and CD37 mAbs induce superior *ex vivo* CDC of tumor cells obtained from patients with B-cell malignancies

We next examined the capacity of combinations of Hx-CD20 and Hx-CD37 mAbs to induce CDC *ex vivo* in tumor cells obtained from patients with B-cell malignancies. First, the CDC activity of Hx-CD20-7D8, Hx-CD37 or combinations was evaluated using tumor cells obtained from 15 patients diagnosed with CLL. Both Hx-CD20-7D8 and Hx-CD37 induced substantial CDC of CLL tumor cells from all 15 tested donors (Figure 6A), in accordance with Figure 1. Hx-CD37 was more effective in CDC than Hx-CD20-7D8, which may

◀ **Figure 5**

Hexamerization-enhanced CD20 and CD37 mAbs cooperate in CDC through Fc-mediated clustering in hetero-hexamers. The effect of introducing Fc-Fc inhibiting mutations S440K and K439E on the CDC induction of hexamerization-enhanced type II CD20 mAb 11B8-derived Hx-CD20-11B8 on Daudi cells (**A**) and WIL2-S cells (**B**), hexamerization-enhanced CD37 mAb 37.3-derived Hx-CD37 on Daudi (**C**) and WIL2-S cells (**D**) and the mAb combinations thereof on Daudi (**E**) and WIL2-S cells (**F**). Cells were opsonized with concentration series of Hx-CD20-11B8 and Hx-CD37 variants in the presence of 20% NHS. CDC induction is expressed as the percentage lysis determined by the fraction of PI-positive cells. Representative examples of two (WIL-2S) and three replicates (Daudi) are shown. (**G**) The effect of introducing Fc-Fc inhibiting mutations S440K and K439E on the molecular proximity of Hx-CD20-11B8 and Hx-CD37 variants on the cell membrane of Daudi cells. Daudi cells were incubated with 10 µg/mL A555-conjugated Hx-CD20-11B8 variants and 10 µg/mL A647-conjugated Hx-CD37 variants for 15 minutes at 37˚C. FRET was calculated from the MFI values as determined by flow cytometry. Data shown are mean and SD of six replicates collected from three independent experiments.

be explained by higher expression CD37 on CLL cells ($P < 0.05$, Supplementary Figure 3A-B). Importantly, significantly increased CDC levels were observed in 9 out of 15 tested CLL donors upon treatment with the combination of Hx-CD20-7D8 and Hx-CD37. Even at modest total concentrations of Hx-CD20-7D8 and Hx-CD37 (Σ 1.25 µg/mL for each mAb), >90% CDC of B cells was induced in 12 out of the 15 tested CLL donors (Figure 6A). Enhanced CDC by the mAb combination was observed over a range of mAb concentrations and at different mAb ratio's, and was more apparent at lower mAb concentrations as illustrated for one representative donor (Figure 6B). Next, we evaluated the cytotoxic capacity of Hx-CD20-11B8, Hx-CD37, and the combination thereof using tumor cells of 10 patients diagnosed with different B-cell lymphomas, including B-NHL (NOS), FL, MZL and MCL. While for the single agents a large variation in CDC efficacy was observed between the donors, the combination of Hx-CD20-11B8 and Hx-CD37 consistently showed enhanced CDC activity compared to the single mAbs (Figure 6C). Representative figures from each tested lymphoma subtype show that combinations of Hx-CD20-11B8 and Hx-CD37 at the tested 1:1 ratio may enhance CDC, even when CDC induced by the individual mAbs was low or absent (Figure 6D). Furthermore, analysis of CD20 and CD37 target expression levels on primary B cells from 24 CLL patients and 10 patients with different NHL subtypes illustrated a large diversity in target expression levels and ratios (Supplementary Figure 3A-C). These results suggest that combinations of Hx-CD20 and Hx-CD37 mAbs may generally increase the therapeutic potential of CDC-inducing mAbs in B-cell malignancies accross different target expression levels and ratios.

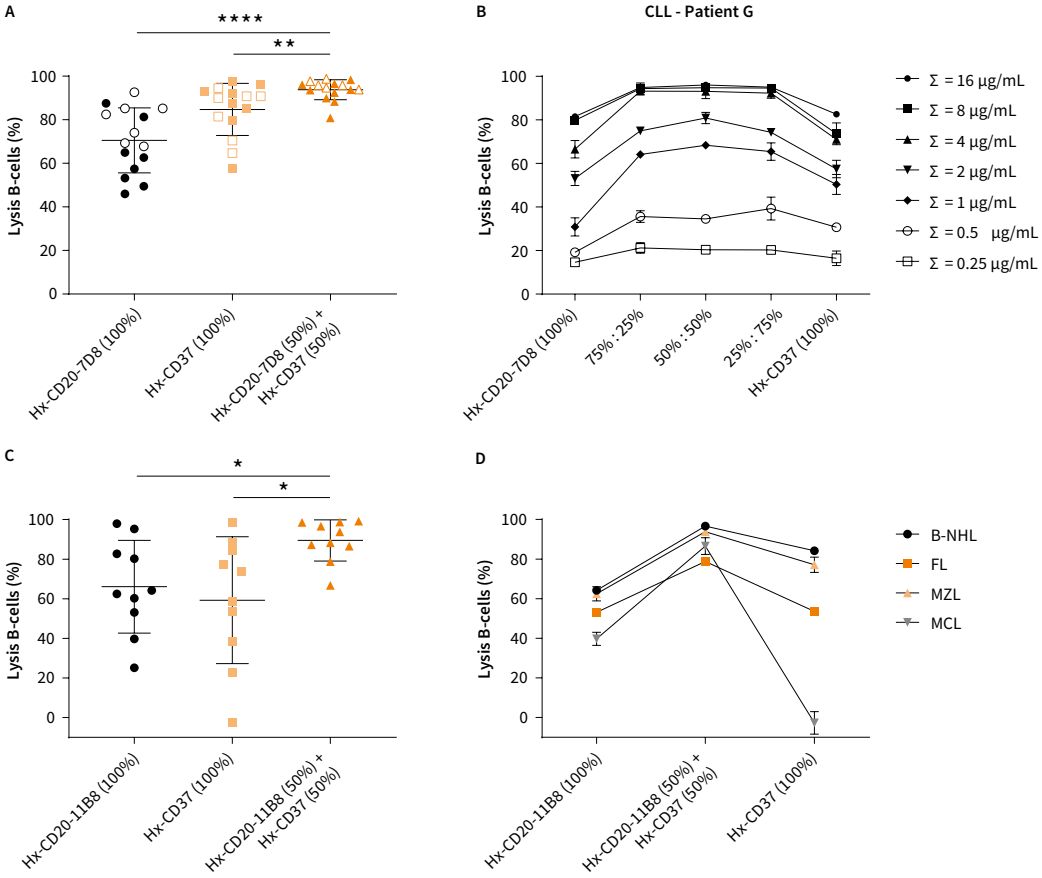

▲ Figure 6

Combinations of hexamerization-enhanced CD20 and CD37 mAbs induce superior ex vivo CDC of tumor cells obtained from patients with B-cell malignancies.

(**A**) B cells obtained from 15 patients diagnosed with CLL were opsonized with fixed concentrations of hexamerization-enhanced type I CD20 mAb 7D8-derived Hx-CD20-7D8 or hexamerization-enhanced CD37 mAb 37.3-derived Hx-CD37 (open symbols: 2.5 µg/mL, closed symbols: 2 µg/mL; each presented as 100%), or 1:1 mixtures thereof (open symbols: 0.625 µg/mL of each mAb, closed symbols: 0.5 µg/mL of each mAb; each represented as 50%) in the presence of 50% NHS. CDC induction is presented as the percentage lysis determined by the fraction of TO-PRO-3 positive cells. (**B**) B cells of a representative CLL patient sample (patient G) were opsonized with different total mAb concentrations of Hx-CD20-7D8 or Hx-CD37 (single agents indicated as 100%) and combinations thereof at different antibody ratios (indicated as 75%:25%, 50%:50% and 25%:75%) in the presence of 50% NHS. CDC induction is presented as the percentage lysis determined by the fraction of TO-PRO-3 positive cells. Data shown are mean and SD of duplicate measurements. (**C**) B cells obtained from 10 patients diagnosed with different B-cell malignancies (B-NHL (NOS), FL, MZL and MCL) were opsonized with 10 µg/mL of hexamerization-enhanced type II CD20 mAb 11B8-derived Hx-CD20-11B8 or Hx-CD37, and the combination thereof (5 + 5 µg/mL) in the presence of 20% NHS. CDC induction is presented as the percentage lysis determined by the fraction of 7-AAD positive B-lymphoma cells. (**D**) CDC assay with B-cell patient samples representative for B-NHL (NOS), FL, MZL and MCL as described in (**C**). Data shown are mean and SD of duplicate measurements.

DISCUSSION

Improving therapeutic efficacy against (heterogeneous) tumors has been the focus of intense preclinical and clinical development. We previously showed that the therapeutic potential of IgG1 mAbs can be enhanced by introducing mutations that improve hexamerization by Fc-mediated clustering and thereby increase CDC activity.[15,16] In the present study, we introduced a Hx mutation, E430G, into CD20 and CD37 mAbs and observed an impressive increase in CDC activity in primary CLL samples. Moreover, combinations of CD20 and CD37 mAbs showed enhanced and synergistic CDC activity, including combinations of Hx-CD37 mAbs with the approved mAbs rituximab, ofatumumab and obinutuzumab. With several CD20 and CD37 mAbs approved or in clinical development, it is attractive to study the mechanism behind the cooperativity between mAbs targeting these two antigens.[34,35] It was recently reported that expression levels of CD20 and CD37 mRNA and protein are correlated on lymphoma B cells.[36] Here, using confocal microscopy and FRET analysis we show that CD20 and CD37 mAbs colocalize on surfaces of B cells and that enhancing Fc-Fc interactions increases mAb colocalization. The observed synergistic CDC activity of CD20 and CD37 mAbs was supported by increased C1q binding and increased CDC efficacy, as illustrated by enhanced CDC at relatively low C1q concentrations. Synergy in complement activation was most evident for CD37 mAbs in combination with type II CD20 mAbs, than with type I CD20 mAbs which are already effective at clustering as WT mAbs.

De Winde et al., [37] recently suggested that the organization of the B-cell plasma membrane is shaped by dynamic protein-protein interactions and that this organization might be altered by targeted mAb therapies. It has previously been described that membrane proteins can cluster into lipid rafts or tetraspanin enriched microdomains (TEMs), enabling efficient signal transduction.[38,39] We hypothesized that the synergistic interactions in CDC between CD20 and CD37 mAbs could be driven by clustering of both target-bound mAbs into oligomeric complexes. By introducing Fc-Fc inhibiting mutations we were able to demonstrate that CD20 and CD37 mAbs do not only permit the formation of homo-hexamers consisting of mAbs bound to either single target separately, but also allow the formation of hetero-hexamers composed of alternating CD20 and CD37 mAbs, each bound to their own cognate target, explaining the synergistic effects. As proposed in Figure 7, other hetero-hexamer variants may occur, although the presence of such alternative variants remains to be demonstrated. We therefore propose a model for Fc-mediated clustering of synergistic mAb combinations on malignant B cells (Figure 7). Upon binding of mAbs targeting two different co-expressed antigens on the

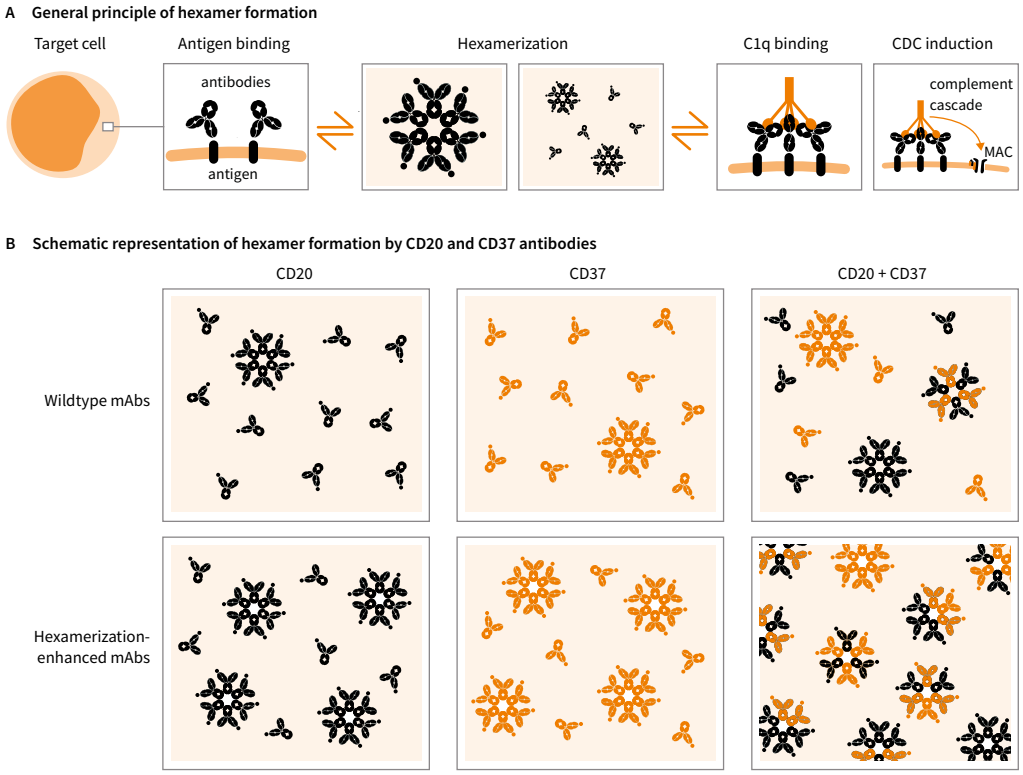

▲ **Figure 7**

Model for Fc-mediated clustering of CD20 and CD37 mAbs in hetero-hexamers upon binding to the cell surface.
(**A**) mAbs naturally cluster into hexameric complexes upon antibody binding to a cognate antigen on a target cell, thereby providing a docking site for C1q binding and CDC induction. (**B**) Upon binding of mAbs targeting two different co-expressed antigens on the plasma membrane that (are able to) colocalize, hetero-hexameric antibody complexes are formed consisting of both mAbs, providing a docking site for C1q binding and CDC induction. Introducing hexamerization-enhancing mutations can increase Fc-mediated clustering of mAbs, both into homo- and hetero-hexameric antibody complexes on the cell surface, thereby increasing the number of C1q docking sites and further potentiating CDC.

plasma membrane that (are able to) colocalize, hetero-hexameric complexes are formed, providing a docking site for C1q binding and CDC induction. Introducing hexamerization-enhancing mutations can increase Fc-mediated clustering of mAbs into both homo- and hetero-hexameric complexes, thereby increasing the number of hexamers and further potentiating CDC. Increasing the therapeutic potency of mAb combinations, driven by hetero-hexamerization, could be of clinical relevance as illustrated by a combination of Hx-CD20 and Hx-CD37 mAbs that showed strong CDC of tumor B cells obtained from patients with different B-cell malignancies. Hicks et al [40] recently reported that the antitumor activity of IMGN529, a CD37-targeting antibody-drug conjugate in clinical development, was potentiated in combination with rituximab *in vivo*

in B-NHL xenograft models, which was associated with increased CD37 internalization rates. Other mechanisms of synergy between CD20 and CD37 have also been reported, such as upregulation of CD20 expression in Daudi cells after treatment with the radiolabeled anti-CD37 mAb ^{177}Lu-lilotomab.[41]

The concept of antibody hetero-hexamer formation may hold relevance for a broader range of targets and effector mechanisms. An emerging therapeutic approach is the development of designer polyclonals, consisting of multiple mAbs in one product of which several are in clinical development, such as MM-151, targeting three epitopes on EGFR and Sym013, a mixture of six mAbs targeting all three HER family members (EGFR, HER2 and HER3).[42,43] One could speculate that enhancing Fc-mediated antibody clustering involving different co-expressing targets on hematologic or solid tumors may induce synergystic efficacy, providing a rationale for application in designer polyclonals. Whether effector mechanisms other than CDC, such as ADCC or ADCP are also enhanced by combinations of CD20 and CD37 mAbs remains to be elucidated. One may speculate that the engagement of two mAbs binding co-expressed targets allows for higher total antibody binding on the cell surface, allowing more efficient engagement of FcγRs on effector cells.

In the present work, we have demonstrated that synergy in CDC induced by combinations of CD20 and CD37 mAbs is likely driven by Fc-mediated clustering into hetero-hexameric antibody complexes on the cell surface. Enhancing hetero-hexamerization between mAb combinations using Fc engineering represents a powerful tool to increase the therapeutic efficacy of mAb combinations directed against hematologic tumor targets, as well as other tumor targets.

REFERENCES

1. Deans JP, Li H, Polyak MJ. CD20-mediated apoptosis: signalling through lipid rafts. *Immunology* 2002; **107**(2): 176-82.

2. Gopal AK, Press OW. Clinical applications of anti-CD20 antibodies. *Transl Res* 1999; **134**(5): 445-50.

3. Leget GA, Czuczman MS. Use of rituximab, the new FDA-approved antibody. *Curr Opin Oncol* 1998; **10**(6): 548-51.

4. Beurskens FJ, Lindorfer MA, Farooqui M, et al. Exhaustion of cytotoxic effector systems may limit mAb-based immunotherapy in cancer patients. *J Immunol* 2012; **188**(7): 3532-41.

5. Taylor RP, Lindorfer MA. Analyses of CD20 Monoclonal Antibody–Mediated Tumor Cell Killing Mechanisms: Rational Design of Dosing Strategies. *Mol Pharmacol* 2014; **86**(5): 485-91.

6. Weiner GJ. Building better monoclonal antibody-based therapeutics. *Nat Rev Cancer* 2015; **15**(6): 361-70.

7. Wang X, Mathieu M, Brezski RJ. IgG Fc engineering to modulate antibody effector functions. *Protein Cell* 2018; **9**(1): 63-73.

8. Lazar GA, Dang W, Karki S, et al. Engineered antibody Fc variants with enhanced effector function. *PNAS* 2006; **103**(11): 4005-10.

9. Richards JO, Karki S, Lazar GA, Chen H, Dang W, Desjarlais JR. Optimization of antibody binding to Fc RIIa enhances macrophage phagocytosis of tumor cells. *Mol Cancer Ther* 2008; **7**(8): 2517-27.

10. Shields RL, Namenuk AK, Hong K, et al. High Resolution Mapping of the Binding Site on Human IgG1 for Fcgamma RI, Fcgamma RII, Fcgamma RIII, and FcRn and Design of IgG1 Variants with Improved Binding to the Fcgamma R. *J Biol Chem* 2000; **276**(9): 6591-604.

11. Stavenhagen JB, Gorlatov S, Tuaillon N, et al. Fc Optimization of Therapeutic Antibodies Enhances Their Ability to Kill Tumor Cells In vitro and Controls Tumor Expansion In vivo via Low-Affinity Activating Fc Receptors. *Cancer Res* 2007; **67**(18): 8882-90.

12. Idusogie EE, Wong PY, Presta LG, et al. Engineered antibodies with increased activity to recruit complement. *J Immunol* 2001; **166**(4): 2571-5.

13. Natsume A, In M, Takamura H, et al. Engineered Antibodies of IgG1/IgG3 Mixed Isotype with Enhanced Cytotoxic Activities. *Cancer Res* 2008; **68**(10): 3863-72.

14. Melis JPM, Strumane K, Ruuls SR, Beurskens FJ, Schuurman J, Parren PWHI. Complement in therapy and disease: Regulating the complement system with antibody-based therapeutics. *Mol Immunol* 2015; **67**(2, Part A): 117-30.

15. Diebolder CA, Beurskens FJ, de Jong RN, et al. Complement Is Activated by IgG Hexamers Assembled at the Cell Surface. *Science* 2014; **343**(6176): 1260.

16. de Jong RN, Beurskens FJ, Verploegen S, et al. A Novel Platform for the Potentiation of Therapeutic Antibodies Based on Antigen-Dependent Formation of IgG Hexamers at the Cell Surface. *PLoS Biol* 2016; **14**(1): e1002344.

17. Lindorfer MA, Cook EM, Tupitza JC, et al. Real-time analysis of the detailed sequence of cellular events in mAb-mediated complement-dependent cytotoxicity of B-cell lines and of chronic lymphocytic leukemia B-cells. *Mol Immunol* 2016; **70**: 13-23.

18. Teeling JL, French RR, Cragg MS, et al. Characterization of new human CD20 monoclonal antibodies with potent cytolytic activity against non-Hodgkin lymphomas. *Blood* 2004; **104**(6): 1793.

19. Dechant M, Weisner W, Berger S, et al. Complement-Dependent Tumor Cell Lysis Triggered by Combinations of Epidermal Growth Factor Receptor Antibodies. *Cancer Res* 2008; **68**(13): 4998.

20. Klausz K, Berger S, Lammerts van Bueren Jeroen J, et al. Complement-mediated tumor-specific cell lysis by antibody combinations targeting epidermal growth factor receptor (EGFR) and its variant III (EGFRvIII). *Cancer Sci* 2011; **102**(10): 1761-8.

21. Link MP, Bindl J, Meeker TC, et al. A unique antigen on mature B cells defined by a monoclonal antibody. *J Immunol* 1986; **137**(9): 3013.

22. Schwartz-Albiez R, Dörken B, Hofmann W, Moldenhauer G. The B cell-associated CD37 antigen (gp40-52). Structure and subcellular expression of an extensively glycosylated glycoprotein. *J Immunol* 1988; **140**(3): 905.

23. Deckert J, Park PU, Chicklas S, et al. A novel anti-CD37 antibody-drug conjugate with multiple anti-tumor mechanisms for the treatment of B-cell malignancies. *Blood* 2013; **122**(20): 3500.

24. Heider K-H, Kiefer K, Zenz T, et al. A novel Fc-engineered monoclonal antibody to CD37 with enhanced ADCC and high proapoptotic activity for treatment of B-cell malignancies. *Blood* 2011; **118**(15): 4159-68.

25. Pereira DS, Guevara CI, Jin L, et al. AGS67E, an Anti-CD37 Monomethyl Auristatin E Antibody–Drug Conjugate as a Potential Therapeutic for B/T-Cell Malignancies and AML: A New Role for CD37 in AML. *Mol Cancer Ther* 2015; **14**(7): 1650-60.

26. Repetto-Llamazares AHV, Larsen RH, Patzke S, et al. Targeted Cancer Therapy with a Novel Anti-CD37 Beta-Particle Emitting Radioimmunoconjugate for Treatment of Non-Hodgkin Lymphoma. *PLoS One* 2015; **10**(6): e0128816.

27. Zhao XB, Biswas S, Mone A, et al. Novel Anti-CD37 Small Modular Immunopharmaceutical (SMIP) Induces B-Cell-Specific, Caspase-Independent Apoptosis in Human CLL Cells. *Blood* 2004; **104**(11): 2515.

28. Burton DR, Pyati J, Koduri R, et al. Efficient neutralization of primary isolates of HIV-1 by a recombinant human monoclonal antibody. *Science* 1994; **266**(5187): 1024.

29. Deckert. J. CD37-binding molecules and immunoconjugates thereof. *WO 2011/112978A1* 2011.

30. Vink T, Oudshoorn-Dickmann M, Roza M, Reitsma J-J, de Jong RN. A simple, robust and highly efficient transient expression system for producing antibodies. *Methods* 2014; **65**(1): 5-10.

31. Cook EM, Lindorfer MA, van der Horst H, et al. Antibodies That Efficiently Form Hexamers upon Antigen Binding Can Induce Complement-Dependent Cytotoxicity under Complement-Limiting Conditions. *J Immunol* 2016; **197**(5): 1762-75.

32. Cragg MS, Morgan SM, Chan HTC, et al. Complement-mediated lysis by anti-CD20 mAb correlates with segregation into lipid rafts. *Blood* 2003; **101**(3): 1045.

33. Chou T-C. Theoretical Basis, Experimental Design, and Computerized Simulation of Synergism and Antagonism in Drug Combination Studies. *Pharmacol Rev* 2006; **58**(3): 621.

34. Beckwith KA, Byrd JC, Muthusamy N. Tetraspanins as therapeutic targets in hematological malignancy: a concise review. *Front Physiol* 2015; **6**: 91.

35. Teo EC-y, Chew Y, Phipps C. A review of monoclonal antibody therapies in lymphoma. *Crit Rev Oncol Hematol* 2016; **97**: 72-84.

36. Xu-Monette ZY, Li L, Byrd JC, et al. Assessment of CD37 B-cell antigen and cell of origin significantly improves risk prediction in diffuse large B-cell lymphoma. *Blood* 2016; **128**(26): 3083-100.

37. de Winde CM, Elfrink S, van Spriel AB. Novel Insights into Membrane Targeting of B Cell Lymphoma. *Trends Cancer* 2017; **3**(6): 442-53.

38. Hemler ME. Tetraspanin functions and associated microdomains. *Nat Rev Mol Cell Biol* 2005; **6**(10): 801-11.

39. Simons K, Sampaio JL. Membrane Organization and Lipid Rafts. *Cold Spring Harb Perspect Biol* 2011; **3**(10): a004697.

40. Hicks SW, Lai KC, Gavrilescu LC, et al. The Antitumor Activity of IMGN529, a CD37-Targeting Antibody-Drug Conjugate, Is Potentiated by Rituximab in Non-Hodgkin Lymphoma Models. *Neoplasia* 2017; **19**(9): 661-71.

41. Repetto-Llamazares AHV, Malenge MM, O'Shea A, et al. Combination of (177) Lu-lilotomab with rituximab significantly improves the therapeutic outcome in preclinical models of non-Hodgkin's lymphoma. *Eur J Haematol* 2018; **101**(4): 522-31.

42. Dienstmann R, Patnaik A, Garcia-Carbonero R, et al. Safety and Activity of the First-in-Class Sym004 Anti-EGFR Antibody Mixture in Patients with Refractory Colorectal Cancer. *Cancer Discov* 2015; **5**(6): 598.

43. Jacobsen HJ, Poulsen TT, Dahlman A, et al. Pan-HER, an Antibody Mixture Simultaneously Targeting EGFR, HER2, and HER3, Effectively Overcomes Tumor Heterogeneity and Plasticity. *Clin Cancer Res* 2015; **21**(18): 4110.

44. Baig NA, Taylor RP, Lindorfer MA, et al. Complement dependent cytotoxicity (CDC) in chronic lymphocytic leukemia (CLL): Ofatumumab enhances alemtuzumab CDC and reveals cells resistant to activated complement. *Leuk Lymphoma* 2012; **53**(11): 2218-27.

45. Kennedy AD, Beum PV, Solga MD, et al. Rituximab Infusion Promotes Rapid Complement Depletion and Acute CD20 Loss in Chronic Lymphocytic Leukemia. *J Immunol* 2004; **172**(5): 3280.

46. Taylor RP, Wright EL, Pocanic F. Quantitative analyses of C3b capture and immune adherence of IgM antibody/dsDNA immune complexes. *J Immunol* 1989; **143**(11): 3626.

47. Manders E. M M, Verbeek F J, Aten J A. Measurement of co-localization of objects in dual-colour confocal images. *J Microsc* 1993; **169**(3): 375-82.

48. Schneider CA, Rasband WS, Eliceiri KW. NIH Image to ImageJ: 25 years of image analysis. *Nat Methods* 2012; **9**(7): 671-5.

SUPPLEMENTARY METHODS AND MATERIALS

Cells

CLL cells were purified from the blood of newly diagnosed CLL patients (University of Rochester), in accordance with standard protocols (University of Rochester Institutional Review Board).[44] Bone marrow mononuclear cells (BMNCs), peripheral blood mononuclear cells (PBMCs) and lymph node suspension cells from patients with B-cell non-Hodgkin lymphoma (B-NHL, not otherwise specified (NOS)), follicular lymphoma (FL), marginal zone lymphoma (MZL) and mantle cell lymphoma (MCL) were obtained from the Amsterdam University Medical Center (Amsterdam, The Netherlands) after written informed consent and stored using protocols approved by the Privacy Review Board of the Netherlands Cancer Registry in accordance with the declaration of Helsinki. BMNCs and PBMCs were isolated by density-gradient centrifugation (Ficoll-Paque PLUS, GE Healthcare) from bone marrow aspirates or peripheral blood samples of lymphoma patients. Lymph node suspension cells were obtained by mechanical dissociation held overnight at 37˚C and filtered using cell strainers. Cells were used in experiments directly or stored in liquid nitrogen until further use.

Reagents

Fluorescein isothiocyanate (FITC) conjugated rabbit anti-human C1q (Dako) was used for flow cytometry experiments. C1q depleted serum and purified human C1q were obtained from Quidel. Mouse anti-human IgM antibody HB57 and mouse anti-human IgG1 mAb HB43 were used as described.[45,46] Pooled normal human serum (NHS; AB positive) was obtained from Sanquin (Amsterdam, The Netherlands). mAbs labeled with Alexa dyes (A488, A555, A594, A647) were reacted with N-hydroxysuccinimidyl–esters following manufacturer's instructions (Molecular Probes).

Cell markers flow cytometry

Cell markers used to define cell populations from patients with B-cell lymphoma: CD45-KO (Beckman Coulter), CD19-PC7 (Beckman Coulter), CD3-V450 (BD), CD5-APC (BD), CD5-PE (Dako), CD10-APC-H7 (BD), CD10-PE (Dako), CD23-FITC (Biolegend), kappa-APC-H7 (BD), kappa-PE (Dako) and lambda-FITC (Emelca Bioscience). Within the CD45+ cell population, B cells were identified as CD3-CD19+ cells. Malignant cells were identified based on clonality by kappa/lambda staining (B-NHL (NOS), MZL). Tumor specific markers were used (when possible) depending on the lymphoma subtype: CD10+ (FL), CD5+CD23- (MCL).

Expression analysis

Expression levels of cellular markers were determined using an indirect immunofluorescence assay (QIFIKIT®, Agilent Technologies) according to the manufacturer's instructions. Briefly, cells were labeled with primary mouse mAbs and incubated, in parallel with QIFIKIT® beads containing a defined number of mAb molecules, with FITC-labeled Polyclonal Goat Anti-Mouse Immunoglobulins F(ab')2. The number of antibody molecules per cell was determined by extrapolating the measured mean fluorescence intensity (MFI) to the calibration curve generated by plotting the MFI of the individual bead populations against the number of mAb molecules per bead.

Förster Resonance Energy Transfer (FRET) analysis

500,000 Daudi cells/well were incubated with 10 µg/mL A555-conjugated donor mAbs and/or 10 µg/mL A647-conjugated acceptor mAbs in 10 mL of RPMI/0.2% BSA in 96-well round-bottom plates for 15 minutes at 37°C. Cells were washed twice, pelleted by centrifugation (3 minutes, 300xg) and resuspended in 200 µL PBST. Mean fluorescence intensities (MFI) were determined by flow cytometry (FACS Canto ll) by recording 10,000 events at 585/42 nm (FL2, donor A488) and ≥670 nm (FL3), both excited at 488 nm, and at 660/20 nm (FL4, acceptor A647), excited at 635 nm. Unquenched donor fluorescence intensity was determined with cells incubated with A555-conjugated donor mAbs, and non-enhanced acceptor intensity was determined with cells incubated with A647-conjugated acceptor mAbs. Proximity-induced FRET was determined by measuring energy transfer between cells incubated with A555-conjugated donor and A647-conjugated acceptor mAbs. MFI values allowed calculation of FRET according to the following equation:

Energy transfer (ET) = FL3(D, A) − FL2(D, A)/a − FL4(D, A)/b, wherein a = FL2(D)/FL3(D), b = FL4(A)/FL3(A), D is donor, A is acceptor and FLn (D, A) = donor + acceptor.[32]

ET values obtained were normalized:

Normalized energy transfer (%) = 100 * ET/FL3(D, A).

Synergy and colocalization analyses

Synergy between combinations of mAbs was determined using Loewe additivity-based combination index (CI) scores calculated by CompuSyn software (ComboSyn Inc., Paramus, NJ), whereby effects were categorized as additive (CI = 1), synergistic (CI < 1) or antagonistic (CI > 1).[33] In brief, synergistic lysis exceeds the level of one mAb plus the predicted fractional lysis induced by the other mAb on the remainder of the cell population.

mAb colocalization was quantified by calculating spatial overlap (Manders' coefficients) between images of cell-bound A488-labeled Hx-CD20-7D8 and cell-bound A594-labeled Hx-CD37 using the colocalization plugin in ImageJ.[47,48]

SUPPLEMENTARY FIGURES AND TABLES

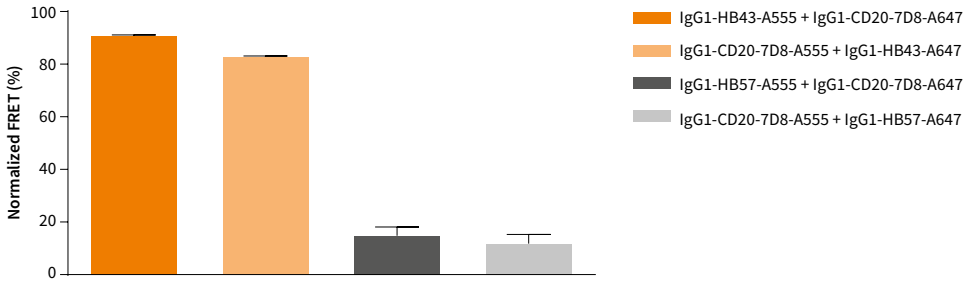

▲ **Supplementary Figure 1**

Evaluation of the dynamic range of fluorescence resonance energy transfer (FRET) detection determined by flow cytometry using control mAbs.

Daudi cells were incubated with 10 µg/mL of A555- or A647-conjugated CD20 mAb 7D8 (IgG1-CD20-7D8) and washed, followed by 10 µg/mL A555- or A647-conjugated mouse-anti-human IgG1 mAb HB43 (IgG1-HB43; positive control) or mouse-anti-human IgM mAb HB57 (IgG1-HB57; negative control) for 15 minutes at 37˚C. FRET was calculated from MFI values as determined by flow cytometry. Data shown are mean and SD of six replicates collected from three independent experiments. IgG1-HB43 was used as a positive control for proximity-induced FRET by virtue of its ability to directly bind, and thus colocalize with a human IgG1 mAb, such as the WT CD20 mAb 7D8 on the cell surface. As binding of A555- or A647-conjugated HB43 requires a cell surface-bound IgG1 mAb, unconjugated IgG1-CD20-7D8 was used for primary binding in the single stainings (calculating the unquenched donor and non-enhanced acceptor fluorescence intensities) and A555- or A647-conjugated IgG1-CD20-7D8 mAb was used for primary binding in the combination stainings (calculating energy transfer efficiency). Using the same setup, IgG1-HB57 was used as a negative control for proximity-induced FRET. HB57 is a murine mAb that binds membrane-bound human IgM (B-cell receptor) on Daudi cells, and was expected to poorly colocalize with the human antibody IgG1-CD20-7D8. Conjugated IgG1-CD20-7D8 and IgG1-HB43 efficiently colocalized with an energy transfer efficiency of 90%, while IgG1-CD20-7D8 and IgG1-HB57 poorly colocalized with ~10% energy transfer efficiency. These data validated the flow cytometry FRET analysis to assess antibody colocalization using A555- and A647-conjugated antibodies.

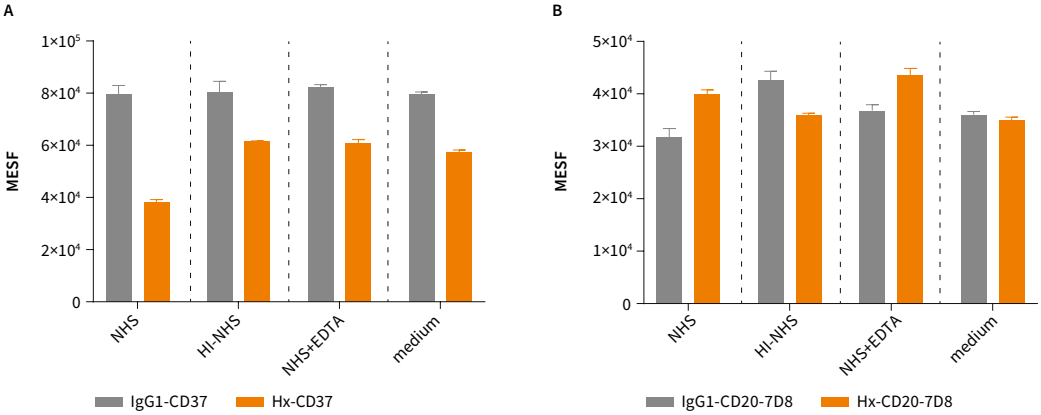

▲ **Supplementary Figure 2**

Binding of CD20 and CD37 mAbs to tumor B cells obtained from a patient diagnosed with CLL (patient A). Antibody binding on primary CLL B cells was analyzed using 16 µg/mL WT CD37 mAb 37.3 (IgG1-CD37) and its hexamerization-enhanced variant Hx-CD37 (**A**) or WT CD20 mAb 7D8 (IgG1-CD20-7D8) and its hexamerization-enhanced variant Hx-CD20-7D8 (**B**) in the presence NHS, HI-NHS, NHS + EDTA or medium. Binding was detected using A488-conjugated mouse anti-human IgG1 Fc mAb HB43 and mean fluorescence intensities were converted to molecules of equivalent soluble fluorochrome (MESF) using calibrated beads (Spherotech). Representative examples of three replicate experiments are shown.

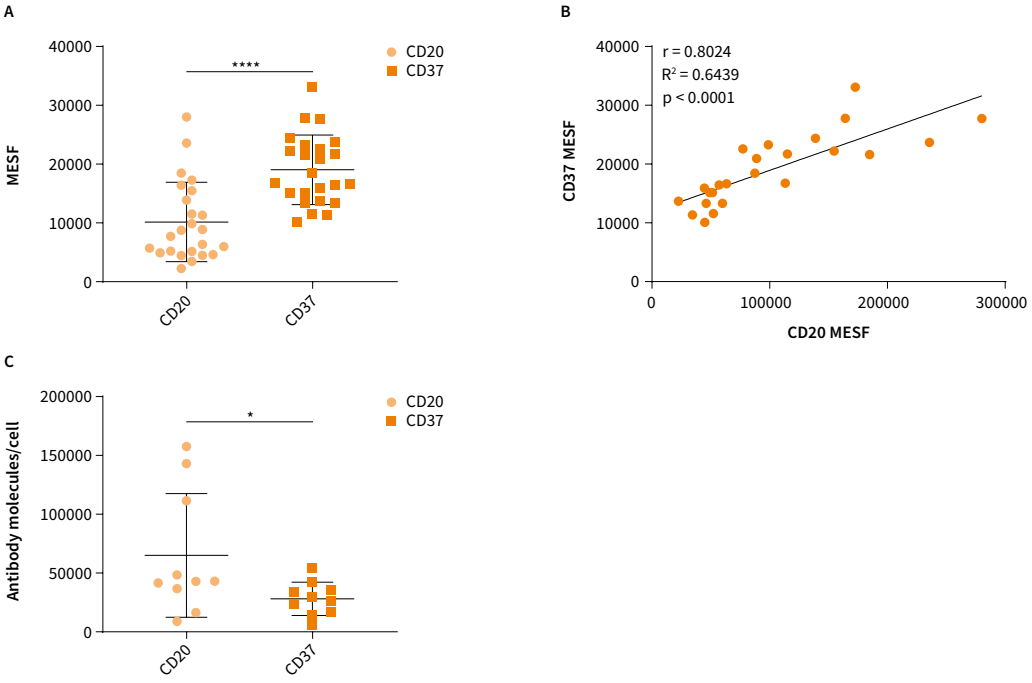

▲ Supplementary Figure 3

CD20 and CD37 target expression levels on tumor B cells obtained from patients with B-cell malignancies.
(**A**) CD20 and CD37 expression. Binding was detected using an A488-conjugated mouse anti-human IgG1 Fc mAb HB43 and mean fluorescence intensities were converted to molecules of equivalent soluble fluorochrome (MESF) using calibrated beads (Spherotech). (**B**) Correlation analysis of CD20 and CD37 expression levels on tumor B cells from 24 CLL patient samples described in (**A**). The Pearson's correlation coefficient (r and R^2) was calculated using GraphPad Prism software. (**C**) CD20 and CD37 expression levels on tumor B cells of 2 B-NHL (NOS), 3 FL, 2 MZL and 3 MCL patient samples. Expression levels were determined using a human IgG calibrator kit (Agilent Technologies). The number of antibody molecules per cell was calculated from the antibody-binding capacity (mean fluorescence intensity) normalized to a calibration curve, according to the manufacturer's guidelines. Significant differences are indicated as *$p < 0.05$ and ****$p < 0.0001$.

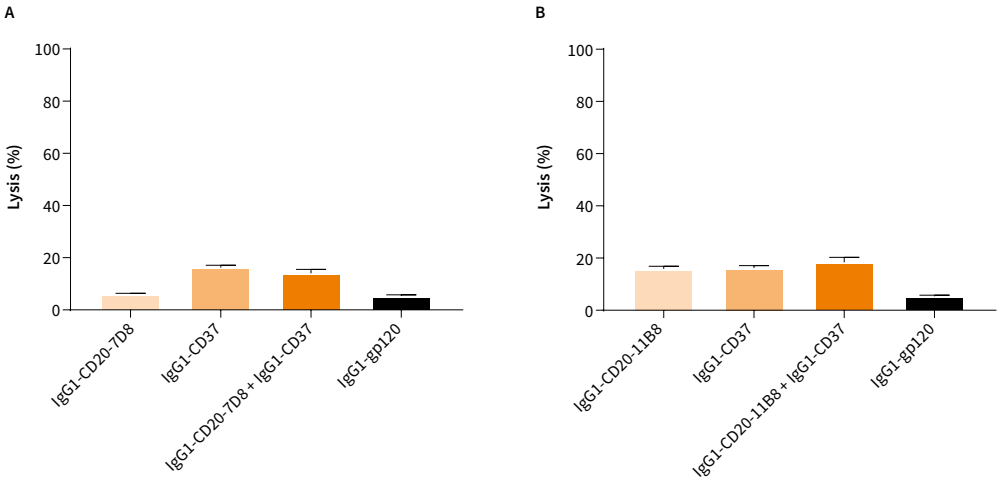

▲ **Supplementary Figure 4**

Minimal cell lysis observed in assays with heat-inactivated serum indicates that cell killing is complement dependent. Daudi cells opsonized with 30 µg/mL WT type I CD20 mAb 7D8 (IgG1-CD20-7D8) (**A**) or WT type II CD20 mAb 11B8 (IgG1-CD20-11B8) (**B**), anti-CD37 mAb 37.3 (IgG1-CD37), or a combination thereof (15 + 15 µg/mL) for 45 minutes at 37°C in the presence of 20% heat-inactivated NHS. HIV gp120-specific mAb b12 (IgG1-gp120) was used as a negative control human mAb. Cell kill is expressed as the percentage lysis determined by the fraction of PI-positive cells. Representative examples of two replicates are shown.

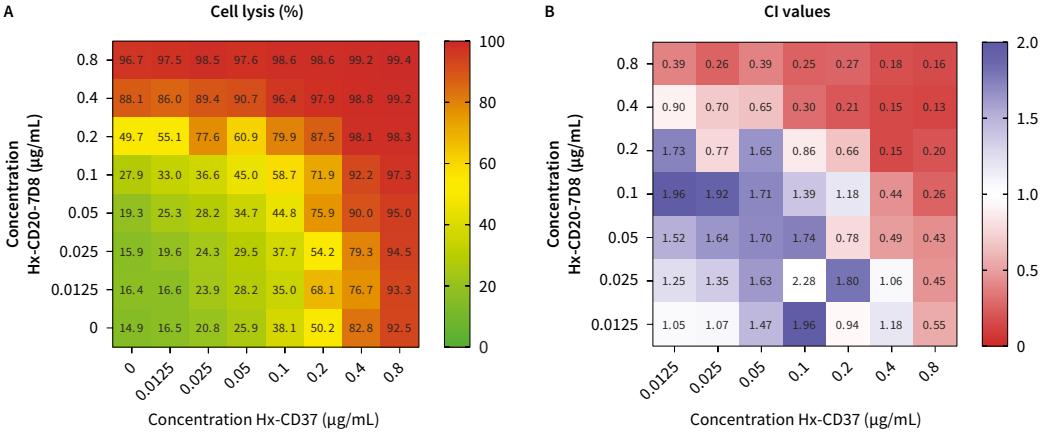

▲ **Supplementary Figure 5**

(**A**) 8 x 8 CDC dose response matrix plot for the combination of hexamerization-enhanced CD37 mAb Hx-CD37 (0-0.8 µg/mL) with hexamerization-enhanced CD20 mAb Hx-CD20-7D8 (0-0.8 µg/mL) tested on Daudi cells and categorized as a color gradient from green (0% lysis) to yellow (50% lysis) to red (100% lysis). HIV gp120-specific mAb b12 (IgG1-gp120) was used as a negative control human mAb. (**B**) Loewe additivity-based Combination index (CI) values calculated by CompuSyn for the CDC dose response matrix as described in (**A**) and categorized as synergistic (<1, red), additive (1, white) and antagonistic (>1, blue). Representative examples of two replicate experiments are shown. CDC induction is expressed as the percentage lysis determined by the fraction of PI-positive cells.

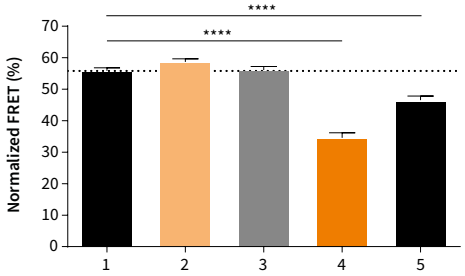

1. Hx-CD37-A555 + Hx-CD20-11B8-A647
2. Hx-CD37-K439E-A555 + Hx-CD20-11B8-S440K-A647
3. Hx-CD37-S440K-A555 + Hx-CD20-11B8-K439E-A647
4. Hx-CD37-K439E-A555 + Hx-CD20-11B8-K439E-A647
5. Hx-CD37-S440K-A555 + Hx-CD20-11B8-S440K-A647

▲ Supplementary Figure 6

The effect of introducing Fc-Fc inhibiting mutations S440K and K439E on the molecular proximity of hexamerization-enhanced CD20 and CD37 mAbs on the cell membrane of Daudi cells.

Daudi cells were incubated with 10 µg/mL A555-conjugated hexamerization-enhanced CD37 mAb 37.3 (Hx-CD37) variants and 10 µg/mL A647-conjugated hexamerization-enhanced CD20 mAb 11B8 (Hx-CD20-11B8) variants for 15 minutes at 37˚C. FRET was calculated from MFI values as determined by flow cytometry. Data shown are mean and SD of six replicates collected from three independent experiments.

	CI values* at different effective doses (ED)			
Antibody Combination	**ED50**	**ED75**	**ED90**	**ED95**
Hx-CD20-7D8 + Hx-CD37	0.96	0.66	0.47	0.37
Hx-CD20-11B8 + Hx-CD37	0.72	0.52	0.39	0.31

* CI values can be categorized as synergistic (<1), additive (=1) and non-synergistic (>1).

▲ Supplementary Table 1

Average Loewe-additivity-based combination index (CI) values calculated by CompuSyn at different effective doses of a CDC dose-response matrix using combinations of hexamerization-enhanced CD20 mAb Hx-CD20-7D8 or Hx-CD20-11B8 with hexamerization-enhanced CD37 mAb Hx-CD37.